

# MOLECULAR SIMULATIONS OF THE FORMATION PROCESS OF FULLERENE

**Yasutaka YAMAGUCHI and Shigeo MARUYAMA**

Dept. of Mech. Engng., The University of Tokyo, 7-3-1 Hongo, Bunkyo-ku, Tokyo 113, Japan

**ABSTRACT.** The formation mechanism of fullerene, a new type of carbon molecule with hollow caged structure, was studied by using the molecular dynamics method with the simplified classical potential function. The clustering process starting from isolated carbon atoms was simulated under controlled temperature condition. Here, translational, rotational and vibrational temperatures of each cluster were controlled to be in equilibrium. The structures of clusters which were obtained after enough calculation depended on the controlled temperature  $T_c$ , yielding the graphitic sheet for  $T_c < 2600$  K, fullerene-like caged structure for  $2600 \text{ K} < T_c < 3500$  K, and chaotic 3-dimensional structure for  $T_c > 3500$  K. Through the detailed trace of precursors, it was revealed that the key feature of the formation of the caged structure was the chaotic 3-dimensional cluster of 40 to 50 atoms which had large vibrational energy. In addition, when the precursors were kept under lower vibrational energy, the successive growth of 2-dimensional graphitic structure was observed. Since the time scale of the simulation was compressed, the annealing process of each cluster was virtually omitted. In order to examine this effect, an imperfect  $C_{60}$  obtained from the similar simulation was annealed at 2500 K for 50 ns without collisions. The perfect Buckminsterfullerene  $C_{60}$  was finally obtained after successive Stone-Wales transformations.

## 1. INTRODUCTION

The existence of soccer-ball structured  $C_{60}$  shown in Fig. 1.1 (a) was demonstrated by Kroto *et al.* (1985) through their time-of-flight mass spectra of carbon clusters generated by the laser-vaporization supersonic-nozzle technique. They observed the prominent  $C_{60}^+$  signal and the complete lack of odd-numbered clusters. They named the cluster  $C_{60}$  of truncated icosahedron Buckminsterfullerene since the beautiful network structure resembled the famous geodesic dome designed by Buckminster Fuller. Since the mass spectra of positive carbon clusters exhibited only even numbered clusters in the range of  $C_{30}$  to at least  $C_{600}$  [Rohlfing *et al.* (1984) and Maruyama *et al.* (1991)], we could speculate that all of those clusters had polyhedral structure. Carbon clusters with such kind of hollow close-caged structure are then called fullerene [Fig. 1.1]. In 1990, discoveries of simple techniques for macroscopic generation and isolation of fullerene by Krätschmer *et al.* (1990),

Haufler *et al.* (1991) and Taylor *et al.* (1990) provided conditions for the application of this kind of new material in many fields. The observation of the superconductivity by Hebard *et al.* (1991) at  $T_c = 18$  K of potassium-doped  $C_{60}$  crystal further accelerated the research field. Within a few years, macroscale amount of metal containing fullerene [Chai *et al.* (1991), Shinohara *et al.* (1992) and Kikuchi *et al.* (1993)], higher fullerenes [Kikuchi *et al.* (1992) and Achiba & Wakabayashi (1993)] and bucky tube in Fig. 1.1(c) [Iijima (1991) and Ebbesen & Ajayan (1992)] were available.

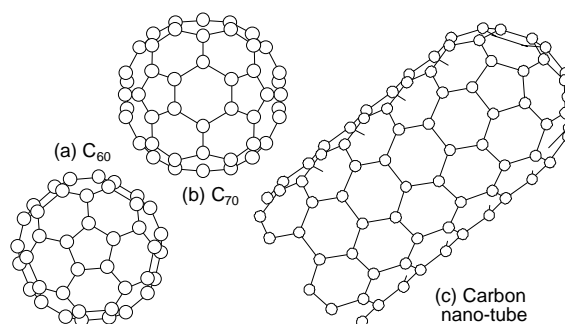


Figure 1.1. Typical structures of fullerene

A common technique of the macroscopic generation of fullerene is to use the arc-discharge method which is simply an arc-discharge of graphite electrodes under a certain pressure of helium buffer gas condition proposed by Haufler *et al.* (1991). The amount of extracted fullerene compared to the collected soot can be yielded up to about 15% under the optimum condition. Usually the generated fullerene consists of 80% of  $C_{60}$ , 15% of  $C_{70}$  and a small amount of higher fullerene like  $C_{76}$ ,  $C_{78}$ ,  $C_{82}$ ,  $C_{84}$ , ..., being some quite interesting magic numbers. It is also surprising that vaporized carbon atoms can automatically form such highly symmetric structures like  $C_{60}$  in the clustering process. Besides these theoretical interests, it is required to clarify the generation mechanism in order to find a more efficient generation method of the higher fullerene or the metal doped fullerene.

Since the macroscale generation technique was found accidentally, the formation mechanism of fullerene is still not clear. Several models have been proposed based on experimental insights. First, Haufler *et al.* (1991) described that the growth of a hexagonal network by successive additions of dimers and trimers eventually left pentagons as the defect. They claimed that the pentagons were essential to give the curvature and to decrease the number of dangling bonds. Because two neighboring pentagons may give too much strain to the network system, then the Isolated Pentagon Rule (IPR) was assumed. It is interesting that the smallest fullerene satisfying IPR is  $C_{60}$  and next to the smallest is  $C_{70}$ . Quite different precursors of fullerene structure were proposed, such as a piece of graphitic sheet [Robertson *et al.* (1992)] or once grown bucky tube [Dravid *et al.* (1993)]. In addition, Heath (1992) proposed a model of clustering sequence from linear chain up to  $C_{10}$ , ring in  $C_{10}$ - $C_{20}$  range, fullerene at  $C_{30}$ . He explained that successive  $C_2$  additions followed until the satisfaction of IPR. Besides these ideas, Wakabayashi & Achiba (1992) proposed a special model that fullerene was made by stacking of carbon rings. The model could explain magic numbers of higher fullerenes [Kikuchi *et al.* (1992) and Achiba & Wakabayashi (1993)] and isomers of  $C_{76}$ ,  $C_{84}$  and  $C_{86}$  [Wakabayashi *et al.* (1993)]. Recently, the drift tube ion chromatography experiments of laser vaporized carbon clusters showed the existence of poly-cyclic rings and the possibility of the annealing of such structure to fullerene [Helden *et al.* (1993), Hunter *et al.* (1993), Clemmer *et al.* (1994) and Hunter *et al.* (1994)].

Although each model can explain some experimental results, it seems to be difficult to decide which model is more plausible. We have applied the molecular dynamics method to simulate the clustering process of carbon atoms in order to speculate the formation process of fullerene from a different point of view. Our previous result [Maruyama & Yamaguchi (1995b)] showed the possibility of simulating the fullerene formation process from randomly distributed carbon atoms. However, since the

temperature control was rather arbitrary, the comparison with the physical phenomena was not easy and no perfect fullerene were obtained. In this study, we performed the similar simulations with more sophisticated temperature control method and considered the importance of annealing.

## 2. MOLECULAR DYNAMICS SIMULATION

The classical molecular dynamics method was employed for the simulation. Two major difficulties were overcome in this simulation. One of them was the assumption of the many-body potential function for carbon atoms. Since the whole process involved the chemical reaction and the bonding of carbon atoms could be varied from  $sp$ ,  $sp^2$  and  $sp^3$ , we could not expect a reliable classical formulation of many-body potential. We employed the potential function developed by Brenner (1990) and ignored the sophisticated conjugate term, because the tough and qualitative function was more plausible than the quantitative but delicate potential function.

Another difficulty was the intrinsic long time scale of the physical process. The laser-vaporization supersonic nozzle experiments suggested that the time scale of the formation of fullerene was about 100 microsecond [Maruyama et al. (1990)]. Probably, the time scale is longer for the arc-discharge method. Then, the direct molecular dynamics simulation of full time scale was far from possible even for the fastest supercomputer. Our choice was to compress the time scale, simply by assuming the high number density of initial carbon atoms. This assumption forced us to modify the boundary conditions and to appreciate the simulated results very carefully. We assumed that the process could be divided into 3 major procedures: 1) Collisions of atoms or clusters each other which would result in the growth of cluster or fragmentation; 2) Cooling of clusters by the continuous collisions with buffer gas molecules and radiation; 3) Annealing of clusters between collisions. The high density meant that the rate of procedure 1) was much increased. Then, we assumed the rate of procedure 2) should be increased accordingly. Because the long time scale of the real system may imply the relatively equilibrium distribution of kinetic energy to translational, rotational and vibrational energy, we used the temperature control method which included the strong tendency toward the equilibrium. Finally, the effect of procedure 3) was underestimated very much. We tried to estimate the effect of the annealing in a separated simulation.

### 2.1 Many-Body Potential Function

We have employed the potential function proposed by Brenner (1990), originally used for his simulation of  $CH_4$  CVD (chemical vapor deposition) of the diamond film. This potential was based on Tersoff's (1986) bond-order expression and was modified to describe the variety of small hydrocarbons, graphite, and diamond lattice. In this potential function, total energy of the system  $E_b$  was described as the sum of the bonding energy of each bond between atom  $i$  and  $j$ .

$$E_b = \sum_i \sum_{j(i>j)} [V_R(r_{ij}) - B_{ij}^* V_A(r_{ij})] \quad (2.1)$$

where  $V_R(r)$  and  $V_A(r)$  were repulsive and attractive force terms, respectively. Morse-type exponential functions with a cut-off function  $f(r)$  were used for these functions.

$$V_R(r) = f(r) \frac{D_e}{S-1} \exp\{-\beta\sqrt{2S}(r-R_e)\} \quad (2.2)$$

$$V_A(r) = f(r) \frac{D_e S}{S-1} \exp\{-\beta\sqrt{2/S}(r-R_e)\} \quad (2.3)$$

$$f(r) = \begin{cases} 1 & (r < R_1) \\ \frac{1}{2} \left( 1 + \cos \frac{r-R_1}{R_2-R_1} \pi \right) & (R_1 < r < R_2) \\ 0 & (r > R_2) \end{cases} \quad (2.4)$$

The state of the bonding was expressed through the term  $B^*$  as the function of angle  $\theta_{ijk}$  between bond  $i-j$  and each neighboring bond  $i-k$ .

$$B^*_{ij} = \frac{B_{ij} + B_{ji}}{2} \quad B_{ij} = \left( 1 + \sum_{k(\neq i,j)} [G_c(\theta_{ijk}) f(r_{ik})] \right)^{-\delta} \quad (2.5)$$

where

$$G_c(\theta) = a_0 \left( 1 + \frac{c_0^2}{d_0^2} - \frac{c_0^2}{d_0^2 + (1 + \cos \theta)^2} \right) \quad (2.6)$$

Since small carbon clusters were not taken into account for Brenner's simulation, the clustering process from small clusters to poly-cyclic bond-network structures could not be simulated [Maruyama & Yamaguchi (1995a)]. In order to avoid it, we ignored the conjugate-compensation term  $F$  which was included in the Brenner's original expression.

Constants were as follows.

$$\begin{aligned} D_e &= 6.325 \text{ eV} & S &= 1.29 & \beta &= 1.5 \text{ \AA}^{-1} & R_e &= 1.315 \text{ \AA} \\ R_1 &= 1.7 \text{ \AA} & R_2 &= 2.0 \text{ \AA} \\ \delta &= 0.80469 & a_0 &= 0.011304 & c_0 &= 19 & d_0 &= 2.5 \end{aligned}$$

Simple Verlet's method was adopted to integrate the equation of motion with its time step of 0.5 fs.

## 2.2 Temperature Control Technique

A cluster was defined as a group of carbon atoms inter-connected one another with C-C bonds. Here, the C-C bond was defined between 2 carbon atoms whose distance was smaller than the cut-off distance  $R_2$ . The kinetic energy of a cluster  $C_n$  with  $n$  carbon atoms was divided into translational, rotational and vibrational energy  $K_T$ ,  $K_R$ ,  $K_V$ , respectively. Each energy was expressed as

$$K_T = \frac{1}{2} nm |\bar{\mathbf{v}}|^2, \quad K_R = \frac{\left| \sum_{i=1}^n m \mathbf{r}'_i \times \mathbf{v}'_i \right|^2}{2 \sum_{i=1}^n m |\mathbf{r}'_i|^2}, \quad K_V = \frac{1}{2} \sum_{i=1}^n m |\mathbf{v}'_i|^2 - K_R \quad (2.7)$$

where,  $m$  was the mass of the carbon atom,  $\mathbf{r}'_i = \mathbf{r}_i - \bar{\mathbf{r}}$  and  $\mathbf{v}'_i = \mathbf{v}_i - \bar{\mathbf{v}}$  were the relative position

and velocity of each atom  $i$  from the mass center position  $\bar{\mathbf{r}} = \frac{1}{n} \sum_{i=1}^n \mathbf{r}_i$  and velocity  $\bar{\mathbf{v}} = \frac{1}{n} \sum_{i=1}^n \mathbf{v}_i$ , respectively. The corresponding temperatures of each cluster and the total system  $T^{\text{total}}$  which was expressed as the weighed average of  $N$  clusters were described as

$$T_T = \frac{2K_T}{3k_B}, \quad T_T^{\text{total}} = \frac{\sum v_T T_T}{\sum v_T} = \frac{2 \sum K_T}{3Nk_B} \quad (2.8)$$

$$T_R = \frac{2K_R}{k_B v_R}, \quad T_R^{\text{total}} = \frac{\sum v_R T_R}{\sum v_R} = \frac{2 \sum K_R}{k_B \sum v_R} \quad (2.9)$$

$$T_V = \frac{2K_V}{k_B v_V}, \quad T_V^{\text{total}} = \frac{\sum v_V T_V}{\sum v_V} = \frac{2 \sum K_V}{k_B \sum v_V} \quad (2.10)$$

where  $v$  was the number of freedom of each motion of a cluster, and  $k_B$  was Boltzmann constant.

As described previously, we tried to enforce the equilibrium of translational, rotational and vibrational temperature of the system in order to incorporate the compression of the time scale by the increase of the number density of carbon atoms. In this calculation, each temperature of the system was independently controlled every 0.1 ps through a simple velocity scaling so that the difference between present temperature of the system and control temperature was reduced to 60 %.

### 3. HIGH TEMPERATURE STABILITY OF C<sub>60</sub>

In order to determine the characteristics of the potential function when applied to fullerene, high temperature stability of the structure of Buckminsterfullerene C<sub>60</sub> [Fig. 1.1 (a)] was examined. Sixty carbon atoms were located at the equilibrium position of the truncated icosahedron C<sub>60</sub> as the initial condition. Then, the vibrational motion was simulated at various temperatures  $T_c$  for 1 ns.

Fig. 3.1 summarizes the observed structure after 1ns at each temperature. For the clarity, the bond-network structures were shown in two-dimensional maps for the hollow caged structures in Fig. 3.1 (a-d). When the temperature was below 2500 K, no change of network structure were observed within 1 ns [Fig. 3.1 (a)]. The shaded pentagons may help to check the characteristics of truncated icosahedron, which has twelve isolated pentagons and 20 hexagons in accordance to (IPR). Slight deformation of the network structure was noticeable for  $T_c = 2600$  K in Fig. 3.1 (b). The isomerization by concerted transformations was observed as discussed later. For  $2600 \text{ K} < T_c < 3000$  K, transformations occurred more frequently but principally keeping the 5-6 network structure. At  $T_c = 3000$  K, dangling bonds for atoms marked by empty symbols were seen as Fig. 3.1 (c). With these dangling bonds, much more violent and continuous reactions were observed. At  $T_c = 3200$  K, several dangling bonds were moving around the network [Fig. 3.1 (d)]. When the temperature was 3500 K, the caged structure was partially broken with a large hole [Fig. 3.1 (e)], and then, transformation to a chaotic 3-dimensional cluster was observed in Fig. 3.1 (f) at  $T_c = 4000$  K. At  $T_c = 5000$  K, a part of cluster was dissociated from the main body [Fig. 3.1 (g)], and when the temperature was as high as 6000 K, the main body could not keep the size and divided into several small clusters [Fig. 3.1 (h)].

Fig. 3.2 shows the detailed process of the transformation of the pentagon-migration observed at 2600 K [Fig. 3.1 (b)]. Until 19.5 ps the network structure kept perfect  $C_{60}$ . From 19.5 ps through 20 ps, bonds marked A-B and C-D were broken and a new bond A-C was created, leaving dangling bonds on atom B and D [Fig. 3.2 (b)]. Then, B chose atom D as a new bond partner at  $t = 20.5$  ps [Fig. 3.2 (c)]. During this process, the lines connecting 4 atoms marked by empty symbols in Fig. 3.2 were merely twisted without any breakage. The whole process could be regarded as a simple migration of pentagons without changing the total number of pentagons and hexagons. This process known as Stone-Wales transformation or pyracylene rearrangement has been argued as a possible path of isomerization of carbon clusters [Stone & Wales (1986)].

We have shown the similar results previously [Maruyama & Yamaguchi (1995b)], where the total energy of the system was kept constant and calculated for 100 ps. The results showed that no isomerization was observed up to 3000 K. Since the difference of temperature control seems to have minor effect in this calculation, the difference of the observation time may be the reason of the discrepancy. If we assume the Arrhenius type of reaction rate for the isomerization process, this discrepancy can be explained that with longer time we have more chance to see the isomerization process. Since the rough activation energy was about 2.5 eV by this simulation, the rough extrapolation of the time scale to seconds ( $10^9$  ns) will give the order of 1000 K for the onset of the isomerization which is in a good agreement with experimental knowledge. Furthermore, it is suggested that the compression of time must be accompanied with the proper increase of temperature in order to reproduce the reasonable reaction.

#### 4. ASSEMBLY OF FULLERENE STRUCTURE

The most interesting point about the formation mechanism of fullerene is how such a hollow caged structure can assembled itself automatically. As seen in the previous section, fullerene structure is extraordinarily stable, even though the 2500 K may be over-estimated. We supposed the high temperature stability would be the key of the preference of fullerene compared to diamond or graphite structure. Although we have already demonstrated that the clustering process of caged

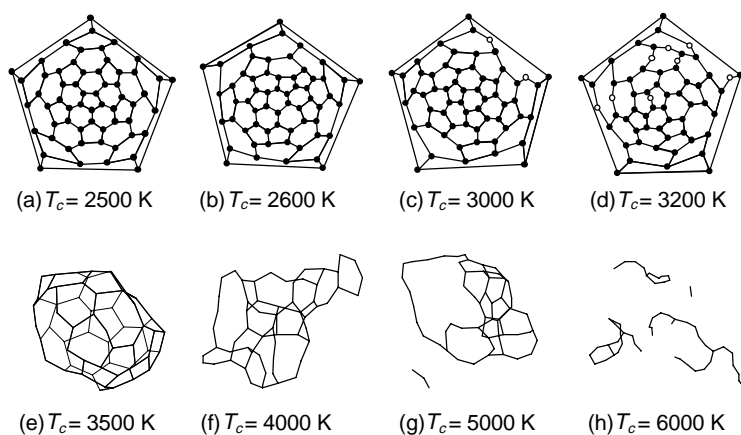


Figure 3.1. High temperature stability of Icosahedral  $C_{60}$

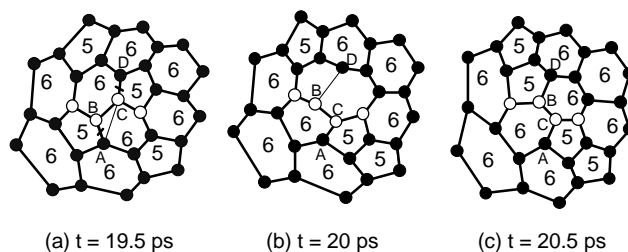


Figure 3.2. Migration of pentagons observed for  $T_c = 2600$  K

structures and flat structures by using this potential function [Maruyama & Yamaguchi (1995b)], it was difficult to evaluate the effect of temperature or density due to the inequilibrium of temperature caused by the previous temperature control method. Then, we applied a new temperature control method and calculated the clustering process under the artificial equilibrium condition.

#### 4.1 Structure of Generated Clusters

As an initial condition, 200 carbon atoms with random velocities were located at random positions in a 8 nm cubic box with full periodic boundary conditions. Then, translational, rotational and vibrational temperature of the system was controlled toward a constant temperature  $T_c$  by the technique described in the previous section. Several snapshots of the simulation for  $T_c = 3000$  K are shown in Fig. 4.1. At 20 ps, most clusters were smaller than  $C_3$ , while several chain clusters as large as  $C_{10}$  were observed. At about  $t = 60$  ps, some of clusters grew to become ring or chain structure with about 12 atoms, and the largest cluster  $C_{25}$  formed a poly-cyclic network structure. A chaotic 3-dimensional structures  $C_{37}$ ,  $C_{45}$ ,  $C_{49}$  and flat structure  $C_{62}$  appeared at  $t = 120$  ps, finally, at  $t = 300$  ps, a large tube-like cluster as large as  $C_{160}$  with hollow caged structure mainly consisted of pentagons and hexagons was obtained. Through the process, the equilibrium of the temperature was realized except for the first 50 ps when the released potential energy was extremely large compared to the cluster size.

Fig. 4.2 shows the representative clusters observed for various temperature conditions after 300 ps calculation. For  $T_c = 1000$  K, the cluster had almost complete 2-dimensional structure though some

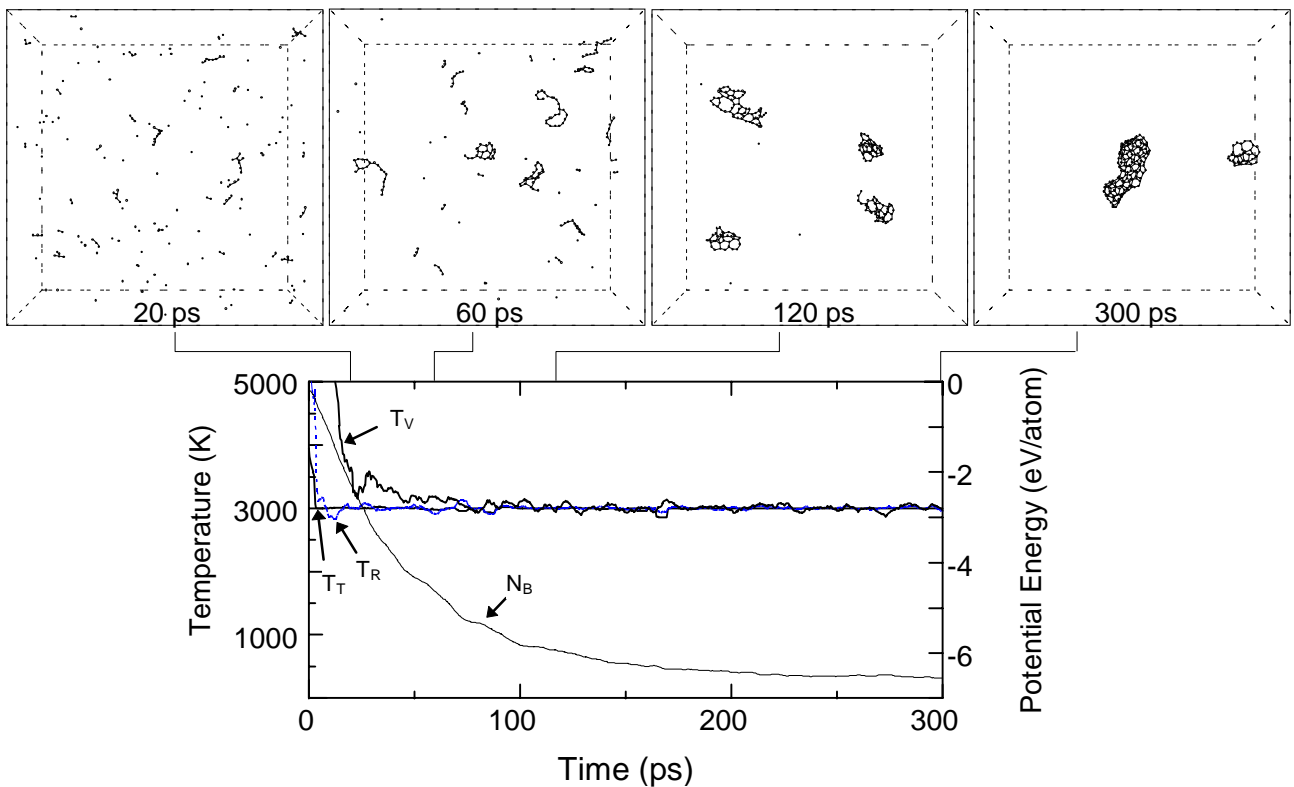


Figure 4.1. Snapshots of clustering process at  $T_c = 3000$ K

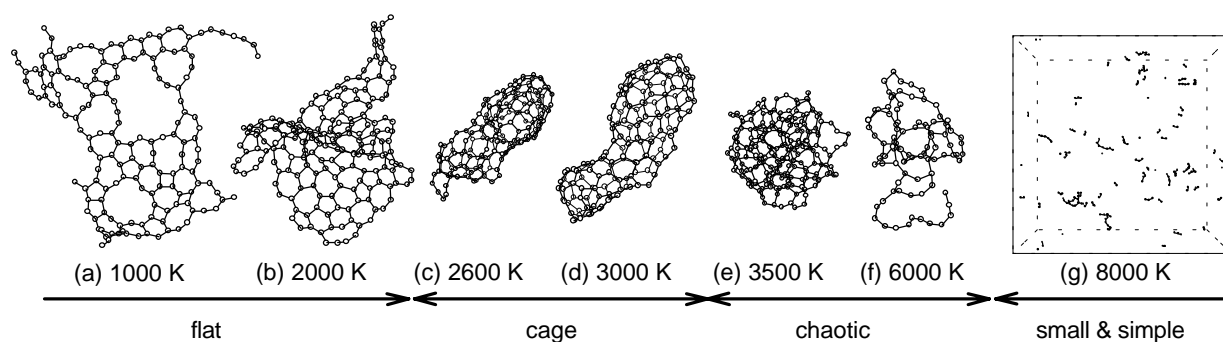


Figure 4.2 Structures of clusters obtained with various temperature control  $T_c$

large rings remained [Fig. 4.2 (a)]. For  $T_c = 2000$  K shown in Fig. 4.2 (b), small poly-cyclic rings coalesced to be a graphitic network structure consisted of two flat components and an irregular part was at the middle. When the control temperature was 2600 K, the cluster constructed an imperfect caged structure with a large hole [Fig. 4.2 (c)]. And for  $T_c = 3000$  K, a hollow caged structure without any large holes was observed [Fig. 4.2 (d)]. For higher temperature as  $T_c = 3500$  K [Fig. 4.2 (e)], the cluster could not keep any regular structure and transform to be a kind of chaotic 3-dimensional structure including some carbon atoms with four bonds. For  $T_c = 6000$  K [Fig. 4.2 (f)], the large clusters could not keep the size due to the thermal dissociation and formed simpler structures. Under very high temperature condition as  $T_c = 8000$  K, the clusters could not grow larger any more and formed some small simple structures such as chains or single rings up to about  $C_{20}$  [Fig. 4.2 (g)].

## 4.2 Precursors in the Reaction Process

The clustering process was examined in detail paying a special attention to the structure and vibrational temperature of precursors. The clustering process yielding a caged structure for  $T_c = 3000$  K are shown in Fig. 4.3 (a). Precursor clusters smaller than  $C_{20}$  had a simple structure basically constructed by chains and a few rings. The coalescence of these small pieces resulted in the random chaotic 3-dimensional structure around  $C_{40}$ . Then, a rather complex transformation to a spherical structure around  $C_{50}$  followed [marked (2) in Fig. 4.3 (a)]. At the same time, another large cluster  $C_{64}$  with a flat graphitic structure was formed. The collision of these two clusters [mark (3) in Fig. 4.3 (a)] and annealing [mark (4) in Fig. 4.3 (a)] resulted in the caged structure of  $C_{160}$ .

The bottom diagram shows the vibrational temperature  $T_v$  and the bond-switching rate  $R_s$  for the marked cluster. The numbers with parentheses on top and bottom panel corresponds to the time periods. Here, the bond switching rate  $R_s$  was defined as the number of bond creation and breakage in a cluster in 1 ps divided by the number of atoms of a cluster. The small clusters with larger vibrational energy frequently switched the bond-network structure, and grew to a larger cluster before the stabilization of the structure [mark (1) in Fig. 4.3 (a)]. The process marked as (2) in Fig. 4.3 (a) shows the rapid annealing and decrease of the bond-switching rate toward  $C_{50}$ . After the middle of the process marked (2), the bond-switching rate become rather smaller compared to the smaller chain and ring clusters, implying the gradual annealing of semi-caged cluster.



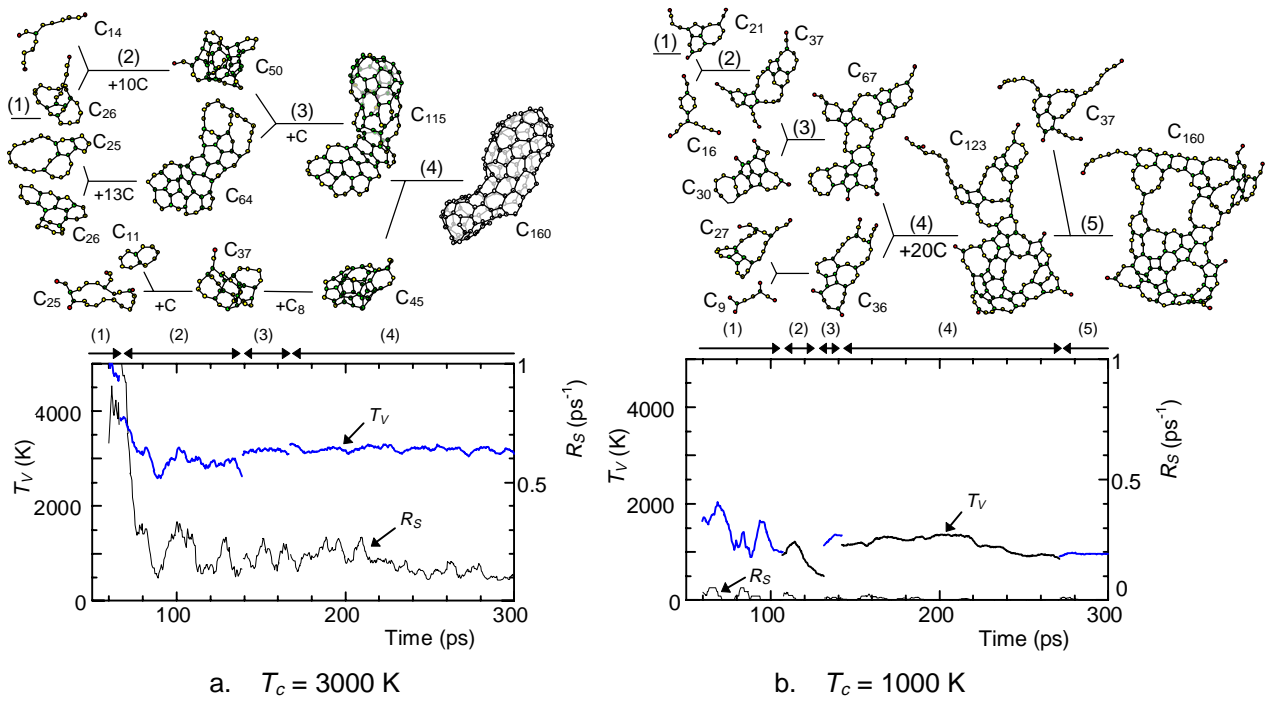


Figure 4.3 Precursors in clustering process

On the other hand, the clustering process yielding a graphitic structure was very simple as shown in Fig. 4.3 (b). At  $T_c = 1000$  K, the precursors always formed flat structure and extended the size in 2-dimensional direction. During the whole process, the clusters had low vibrational temperature and changed the network structure only in the case of the collisions and only around the contact point to organize the flat structure.

### 4.3 Transition of Cluster Size Distribution

Although the selectivity of the caged structure in the certain temperature range has been explained in the previous section, it is still unknown why  $C_{60}$  is so preferable to other sized fullerene. About 80 % of generated fullerene are  $C_{60}$  for typical arc-discharge method. In addition, the percentage of  $C_{60}$  in fullerenes generated from laser-vaporization cluster source is usually less than 0.1 %. The key mechanism of selecting  $C_{60}$  may explain this difference. We considered that the annealing of clusters could give a hint to this problem. The simulation shown in Fig. 4.3 (a) may not be regarded as a successful one, because the final collisions of  $C_{50}$  size range clusters have made too large cluster  $C_{160}$ .

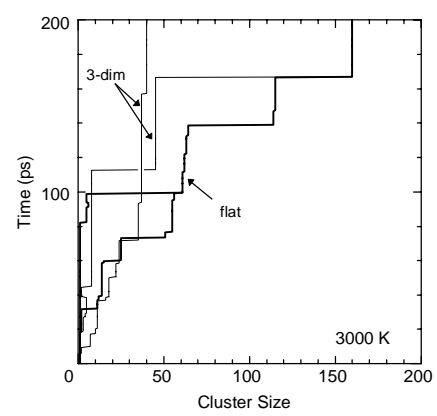


Figure 4.4. Transition of cluster size distribution

In order to estimate the time for annealing, we considered the collisional rate and collisional cross section of each cluster. The time traces of typical large clusters obtained for  $T_c = 3000$  K are shown in Fig. 4.4. Long vertical lines apparent in the figure mean the collision free periods. These long lines appeared when the cluster size grew to about  $C_{40} - C_{60}$ , especially with 3-dimensional structure. This

is related to the decrease of the collisional cross-section by the transformation to the compact 3-dimensional structure. As a consequence, these 3-dimensional clusters can get enough time for annealing toward the perfect fullerene structure which would be stable enough to reject further reactions even with later collisions.

## 5. EFFECT OF ANNEALING

Considering the time scale compression in this simulation, the time scale of the annealing process appeared in Fig. 4.4 can correspond to tens of micro-seconds in practice. In order to evaluate the effect of annealing process, we picked up an imperfect  $C_{60}$  caged cluster obtained in our previous similar simulation [Maruyama & Yamaguchi (1994)], and simulated the annealing process without collisions. The temperature was controlled at  $T_c = 3000$  K for first 8 ns to promote the annealing speed, then set for  $T_c = 2500$  K for about 50 ns. Some snapshots of bond-network structure are summarized in Fig. 5.1. Here, shaded and empty faces are pentagons, and hexagons, respectively, heptagonal faces are marked as 7, empty symbols are atoms with dangling bond. The initial cluster included 4 dangling bonds and 8 heptagons [Fig. 5.1 (a)]. The number of these defects gradually decreased until 15 ns [Fig. 5.1 (c)], where all dangling bonds were terminated and no heptagons remained. A clear correspondence can be seen in the potential energy per atom in the bottom picture. Then, the bond-network could gradually changed through Stone-Wales transformation without the inclusion of heptagons or dangling bonds. However, there were more violent reconstruction of whole network structures at about 18 ns [Fig. 5.1 (c)] and 34 ns. There were only successive Stone-Wales transformations after about 37 ns [Fig. 5.1 (e)] toward the final perfect Buckminsterfullerene  $C_{60}$  in Fig. 5.1 (f). We believe that the violent reconstruction is due to a little too high temperature of the simulation and is not necessary for the real physical annealing process.

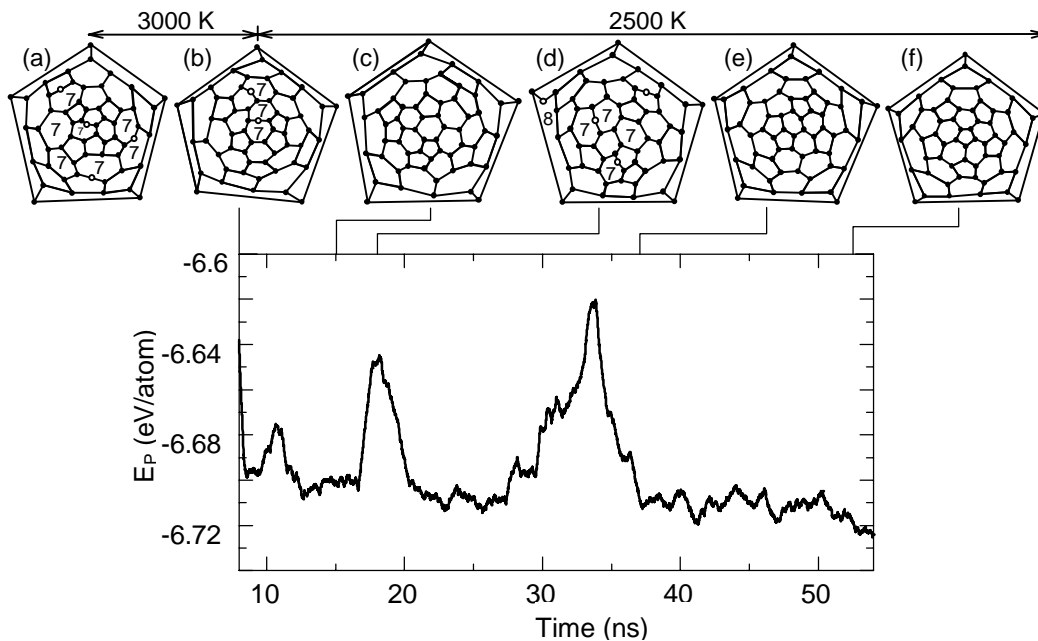


Figure 5.1. Annealing process to perfect  $C_{60}$

## 6. CONCLUSIONS

A molecular dynamics simulation of the clustering process starting from randomly distributed carbon atoms yielded the imperfect fullerenes under certain high temperature conditions. On the other hand, flat graphitic sheet were generated under low temperature condition. The caged structure was shaped through the annealing of chaotic 3-dimensional precursors around  $C_{50}$  with small surface area, in contrast with the consecutive growth mechanism of graphitic sheet. The 3-dimensional clusters around  $C_{50}$  could form a more sophisticated structure through their long lifetime due to the small collisional cross section. Although the simplified potential and the time-scale compression technique due to the computational limitation made it difficult to compare the simulation with experimental results, we could demonstrate that the formation of fullerene was simulated completely through the self-assembly of carbon atoms. Furthermore, the annealing process to the perfect Buckminsterfullerene  $C_{60}$  was demonstrated. These results may suggest the possible path of clustering to fullerene.

## NOMENCLATURE

$B^*$ :	Normalized bond order function	$T_c$ :	Control temperature
$D$ :	Potential well depth	$t$ :	Time
$E_b$ :	Bonding energy	$V_A$ :	Attractive term
$f$ :	Cut-off function	$V_R$ :	Repulsive term
$K$ :	Kinetic energy	$\mathbf{v}$ :	Velocity vector
$k_B$ :	Boltzmann constant		
$m$ :	Mass of carbon		Greek Symbols
$n$ :	Number of molecules of a cluster	$\beta$ :	Potential parameter
$R_s$ :	Bond switching rate	$\delta$ :	Potential parameter
$R_e$ :	Equilibrium bond length	$\nu$ :	Number of freedom of cluster's motion
$R_1$ :	Cut-off distance parameter	$\theta$ :	Angle
$R_2$ :	Cut-off distance parameter		
$r_{ij}$ :	Distance between atom $i$ and atom $j$		Subscripts
$\mathbf{r}$ :	Position vector	$R$ :	Rotational or repulsive
$S$ :	Potential parameter	$T$ :	Translational
$T$ :	Temperature	$V$ :	Vibrational

## ACKNOWLEDGMENTS

We thank Professor Emeritus Susumu Kotake at the University of Tokyo for his kind discussions during this study. This work was supported by a Grant-in-Aid for Scientific Research from the Ministry of Education, Science and Culture, Japan.

## REFERENCES

- Achiba, Y. & Wakabayashi, T., 1993, "Stability, Structures and Hypothetical Growth Mechanism of Carbon 5/6 Network," *Z. Phys. D*, **26**, 69-73.
- Brenner, D. W., 1990, "Empirical Potential for Hydrocarbons for Use in Simulating the Chemical Vapor Deposition of Diamond Films," *Phys. Rev. B*, **42**-15, 9458-9471.

- Chai, Y. *et al.*, 1991, "Fullerenes with Metals Inside," *J. Phys. Chem.*, **95**, 7564-7568.
- Clemmer, D. E. *et al.*, 1994, "Gas-Phase Self-Assembly of Endohedral Metallofullerenes," *Nature*, **367**, 718-720.
- David, V. P. *et al.*, 1993, "Buckytubes and Derivatives: Their Growth and Implications for Buckyball Formation," *Science*, **259**, 1601-1604.
- Ebbesen, T. W. & Ajayan, P. M., 1992, "Large-Scale Synthesis of Carbon Nanotubes," *Nature*, **358**, 220-222.
- Haufler, R. E. *et al.*, 1991, "Carbon Arc Generation of C<sub>60</sub>," *Mat. Res. Soc. Symp. Proc.*, **206**, 627-638.
- Heath, J. R., 1992, "Synthesis of C<sub>60</sub> from Small Carbon Clusters, A Model Based on Experiment and Theory," *Fullerenes*, Ed. G. S. Hammand & V. J. Kuck, American Chemical Society (Washington, D. C.), 1-23.
- Hebard, A. F. *et al.*, 1991, "Superconductivity at 18K in Potassium-Doped C<sub>60</sub>," *Nature*, **350**, 600-601.
- Iijima, S., 1991, "Helical Microtubules of Graphitic Carbon," *Nature*, **354**, 56-58.
- Helden, G. *et al.*, 1993, "Experimental Evidence for the Formation of Fullerenes by Collisional Heating of Carbon Rings in the Gas Phase," *Nature*, **363**, 60-63.
- Hunter, J. *et al.*, 1993, "Annealing C<sub>60</sub><sup>+</sup>: Synthesis of Fullerenes and Large Carbon Rings," *Science*, **260**, 784-786.
- Hunter, J. M. *et al.*, 1994, "Annealing Carbon Cluster Ions: A Mechanism for Fullerene Synthesis," *J. Phys. Chem.*, **98**-7, 1810-1818.
- Kikuchi, K. *et al.*, 1992 "Isolation and Identification of Fullerene Family: C<sub>76</sub>, C<sub>78</sub>, C<sub>82</sub>, C<sub>84</sub>, C<sub>90</sub> and C<sub>96</sub>," *Chem. Phys. Lett.*, **188**-3,4, 177-180.
- Kikuchi, K. *et al.*, 1993 "Isolation and Characterization of the Metallofullerene LaC<sub>82</sub>," *Chem. Phys. Lett.*, **216**-1,2, 23-26.
- Krättschmer, W. *et al.*, 1990, "Solid C<sub>60</sub>: a new form of carbon," *Nature*, **347**, 354-358.
- Kroto, H. W. *et al.*, 1985, "C<sub>60</sub>: Buckminsterfullerene," *Nature*, **318**-6042, 162-163.
- Maruyama, S. *et al.*, 1990, "Direct Injection Supersonic Cluster Beam Source for FT-ICR Studies of Clusters," *Rev. Sci. Instrum.*, **61**-12, 3686-3693.
- Maruyama, S. *et al.*, 1991, "Thermionic Emission from Giant Fullerenes," *Z. Phys. D*, **19**, 409-412.
- Maruyama, S. *et al.*, 1994, "A Molecular Dynamics Simulation for the Formation Mechanism of Fullerene," *Proc. 31st National Heat Transfer Conf.*, 940-941.
- Maruyama, S. & Yamaguchi, Y., 1995a, "A Molecular Dynamics Simulation for the Formation Process of Fullerene (Part 2)," *Proc. 32nd National Heat Transfer Conf.*, 839-840.
- Maruyama, S. & Yamaguchi, Y., 1995b, "A Molecular Dynamics Simulation for the Formation Mechanism of Fullerene," *Therm. Sci. & Engng.*, **3**-3,105-109.
- O'Brien S. C. *et al.*, 1988, "Photophysics of Buckminsterfullerene and Other Carbon Cluster Ions," *J. Chem. Phys.*, **88**-1, 220-230.
- Robertson, D. H. *et al.*, 1992, "On the Way to Fullerenes: Molecular Dynamics Study of the Curling and Closure of Graphitic Ribbons," *J. Phys. Chem.*, **96**, 6133-6135.
- Rohlfing, E. A. *et al.*, 1984, "Production and Characterization of Supersonic Carbon Cluster Beams," *J. Chem. Phys.*, **81**-7, 3322-3330.
- Shinohara, H. *et al.*, 1992 "Mass Spectroscopic and ESR Characterization of Soluble Yttrium-Containing Metallofullerenes YC<sub>82</sub> and Y<sub>2</sub>C<sub>82</sub>," *J. Phys. Chem.*, **96**, 3571-3573.
- Smalley, R. E., 1993, "From Dopyballs to Nanowires," *Materials Science and Engineering*, **B19**, 1-7.
- Stone, A. J. & Wales, D. J., 1986, "Theoretical Studies of Icosahedron C<sub>60</sub> And Some Related Species" *Chem. Phys. Lett.*, **128**, 501-503.
- Taylor, R. *et al.*, 1990, "Isolation, Separation, and Characterization of the Fullerenes C<sub>60</sub> and C<sub>70</sub>: The Third Form of Carbon," *J. Chem. Soc. Chem. Communications*, **1423**, 1423-1425.
- Tersoff, J., 1986, "New Empirical Model for the Structural Properties of Silicon," *Phys. Rev. Lett.*, **56**-6, 632-635.
- Wakabayashi, T. & Achiba, Y., 1992, "A Model for the C<sub>60</sub> and C<sub>70</sub> Growth Mechanism," *Chem. Phys. Lett.*, **190**-5, 465-468.
- Wakabayashi, T. *et al.*, 1993, "A Selective Isomer Growth of Fullerenes," *Chem. Phys. Lett.*, **201**-5,6, 470-474.